
Original Paper

CFD Analysis for Aligned and Misaligned Guide Vane Torque Prediction and Validation with Experimental Data

Christophe Devals¹, Thi C. Vu² and François Guibault¹

¹Department of Computer Engineering, École Polytechnique de Montréal
CP 6079, succ. Centre-ville, Montréal, (QC), H3C 3A7, Canada, christophe.devals@polymtl.ca,
francois.guibault@polymtl.ca

²Andritz Hydro Ltd
6100 Transcanadienne, Pointe-Claire, H9R 1B9, Canada, thi.vu@andritz-hydro.com

Abstract

This paper presents a CFD-based methodology for the prediction of guide vane torque in hydraulic turbine distributor for aligned and misaligned configurations. A misaligned or desynchronized configuration occurs when the opening angle of one guide vane differs from the opening angle of all other guide vanes, which may lead to a torque increase on neighbouring guide vanes. A fully automated numerical procedure is presented, that automates computations for a complete range of operation of a 2D or 3D distributor. Results are validated against laboratory measurements.

Keywords: Torque, Guide Vane, CFD, Casing, Distributor.

1. Introduction

Hydraulic turbine guide vanes control the turbine flow rate by varying their opening positions and, at the same time, provide swirling flow into the runner. The guide vanes are operated by either single or multiple hydraulic servo-motors, depending upon the manufacturer's design. For safe operation, when a single servo-motor is used, the guide vanes are connected to a regulating ring by shear pins. A shear pin is a mechanical safety device that breaks when too much torque is applied on a guide vane. By doing so, the shear pins protect the guide vanes and related mechanism against major damage in emergency cases where the guide vane flow passage is blocked by debris during closure. The guide vane with the broken shear pin could be at any position while all other guide vanes can be operated as required. In such a situation, when one guide vane is in desynchronized mode, the flow behaviour in the casing-distributor is greatly affected by the open flow passage around the broken pin guide vane. The torque on adjacent guide vanes can be very different from the one of normal operation. The knowledge of the guide vane torques of a distributor in desynchronized mode is essential during early design stage. Such information is traditionally obtained by guide vane torque measurements in the hydraulic laboratory. The routine procedure of measuring the guide vane torques in desynchronized mode is to keep the desynchronized guide vane at a fixed opening, usually the first guide vane behind the casing baffle, and to regulate all other guide vanes at different opening angles to cover a whole range of turbine operating conditions. The same procedure is repeated for a series of desynchronized guide vane openings from very small to maximum opening angle. The process is tedious and time consuming. Depending on the number of operating conditions to be investigated, it could take up to several days to complete guide vane torque measurements.

The prediction of the guide vane torque in synchronized and desynchronized mode could be obtained by means of CFD simulation in a casing-distributor assembly. A few references on the casing flow simulation can be found, for instance in [1-8], but no one has treated the subject of desynchronized guide vane torque prediction through numerical simulations. In the last few years, simulations of misaligned guide vanes [5-8] have become a subject of interest in order to improve the stability of pump-turbines at no-load condition. Guide vane torque has been studied experimentally in [9], but the main focus of that paper was on the fluid structure coupling for guide vanes in a pump turbine scale model. One experimental paper has been found for the prediction of misaligned guide vane torque [10]. It showed results of hydraulic torque acting on a misaligned guide vane. It was found that the torque acting on a misaligned guide vane and neighboring vanes is larger than torque in synchronized mode. Vu and Shyy in [11] compared experimental and numerical predictions of total energy loss and synchronized guide vane torque in a two-dimensional turbulent flow analysis of a radial inflow turbine distributor. They showed that 2D flow analysis could predict quite well the flow behavior and performance of the distributor. A similar study was performed in [12]. It dealt with the numerical prediction of pressure distribution and hydraulic torque on guide vane.

Received February 10 2015; revised April 2 2015; accepted for publication April 16 2015: Review conducted by Prof. Yoshinobu Tsujimoto. (Paper number O15006C)

Corresponding author: François Guibault, Professor, francois.guibault@polymtl.ca

However, calculations were performed with a 2D laminar code, but it gave satisfactory results.

The present paper is an extension to the study presented at the 26th IAHR Symposium on Hydraulic Machinery and Systems in 2012 [13]. It describes a methodology based on CFD to assess and validate guide vane torque in desynchronized mode. The paper is structured as follows:

First, the laboratory torque measurement procedure is described in section 2. Next the proposed CFD methodology for automatic meshing and flow simulation for the prediction of torques of a hydraulic turbine guide vane in synchronized and desynchronized mode is introduced in section 3. The following section 4 briefly presents a mesh sensitivity study to determine adequate mesh density for all simulations. Section 5 presents and discusses validation of the guide vane torque prediction with measurements obtained from Andritz Hydro's laboratory for synchronized mode. Calculations are performed both in 2D and 3D. Section 6 presents a validation of the guide vane torque prediction for the distributor in desynchronized mode, and the paper ends with conclusions.

2. Guide vane torque measurement in the hydraulic laboratory

The guide vane torque tests are performed for the distributor in synchronized and desynchronized modes at various speed coefficients, including runaway speed, under non-cavitating conditions. The turbine model usually has a throat diameter of 350 mm and the turbine head can vary from 10 m to 30 m depending on the turbine type for the project. The Reynolds flow number based on throat diameter in the turbine can vary from 1 to 3 million.

The non-dimensional guide vane torque coefficient (CT_2) is expressed as follows:

$$CT_2 = \frac{T_{gv}}{\rho g H_n H_{dist} \left(\frac{\pi D_{gv}}{N_{gv}} \right)^2}, \quad (1)$$

where T_{gv} is the torque on an individual guide vane, ρ is the density of water, g is the gravity, H_n is the turbine head, H_{dist} is the distributor height, D_{gv} is the diameter of the guide vane pivot and N_{gv} is the number of guide vanes.



Fig. 1 Model guide vane equipped with instrumented stem

In practice, the guide vane torque measurement is not performed for all guide vanes in the turbine distributor, but for only a selected few. During model testing, the guide vane torque is measured using stems equipped with strain gauges. Figure 1 shows an instrumented stem bolted to a model guide vane. The instrumented guide vane is calibrated in the laboratory and the measured torque uncertainty without considering the bearing friction in the distributor assembly is about 1.9%. The bearing friction tolerance based on the maximum calibrated guide vane torque is found to be 11.6%. If we include the bearing friction tolerance, the measured torque uncertainty can come up to 13.5%.

For validation purposes we select two project test cases. The first test case is a spiral casing having a distributor height/throat diameter ratio (HD_{ratio}) of 0.225 and the second spiral casing test case has HD_{ratio} equal to 0.3. The validation of the guide vane torque in synchronized mode is carried out with experimental data obtained from test cases #1 and #2. The validation of the guide vane torque in desynchronized mode is performed with measurements from test case #1.

3. Mesh generation and CFD setup

To predict guide vane torque in a distributor in synchronized mode, the use of the distributor geometry only as computational flow domain would be adequate. But for desynchronized mode, the inclusion of the casing in the computational flow domain is necessary. For the present paper, the computational flow domain, as shown in Fig. 2, comprises the spiral casing with all the stay vanes and guide vanes. No runner was taken into account except in section 6.3. The challenge in the meshing for such geometry is the capability to automatically generate, without human intervention, distributor meshes in desynchronized mode containing guide vanes with different opening positions and also for small guide vane openings at the near closing position. In order to facilitate the meshing task, we divide the flow domain into two sub-domains; one for the spiral casing; and the other for the distributor. In-house automatic grid generators providing hexahedral and prismatic elements are used to generate the meshes for both components. The distributor mesh has to be generated for every change in guide vane opening position while the casing mesh is generated once. In order to accommodate the meshing for different guide vane positions from closing to full opening, the distributor mesh contains concentrated hexahedral elements in the vicinity of the vane profiles to resolve the flow boundary layer and prismatic elements in the flow field. The technology on this type of hybrid mesh can be found in [14-15]. The spiral casing mesh contains only hexahedral elements.

To study the mesh sensitivity we generate five different mesh sizes. The number of nodes for the five casing mesh sizes is approximately 0.6M, 1.3M, 2.8M, 3.8M and 7.0M. The number of nodes for the five distributor mesh sizes is approximately 1.1M, 3.4M, 5.6M, 7.8M and 12.5M. All meshes are intended to be used with the $k-\epsilon$ turbulence model, which requires a y^+ value varying from 30 to 100 for the first node near solid walls. For all meshes, the y^+ values are between 57 to 114. The scalable wall function from ANSYS-CFX flow solver is used. Figure 2 illustrates a typical casing-distributor medium size mesh with 4.6M nodes.

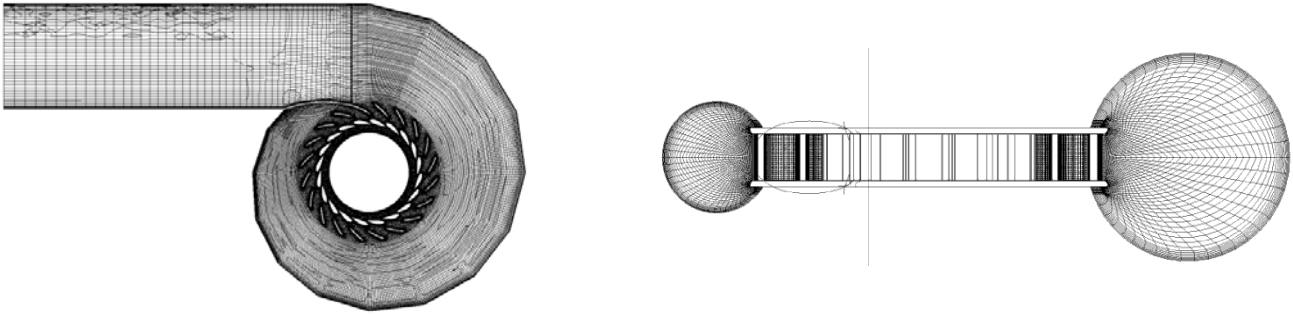


Fig. 2 Casing-distributor mesh – left) Plan view $z = 0$ – right) Section view $y = 0$

The commercial flow solver ANSYS CFX v13.0 is used for the steady state flow analysis with the standard $k-\epsilon$ model. All computations were performed using the high resolution scheme for the momentum equations, and the first order upwind scheme for the turbulent advection equations. The convergence criterion was set to 1×10^{-5} on the root mean square (RMS) residuals for all primitive variables. A maximum of 500 iterations has been imposed for all computations. The connection between the casing and the distributor flow domain is modeled using a General Grid Interface (GGI). A uniform flow with constant inlet velocity is specified at the casing inlet. Average static pressure is prescribed at the distributor outlet boundary. In order to allow the uniform flow from the casing inlet to be fully developed, an extension box, with an equivalent length of three times the throat diameter, is added upstream of the casing inlet.

4. Mesh sensitivity study

We use test case #1 for the study of mesh sensitivity. The flow simulation for the distributor in synchronized mode at 28° guide vane opening is performed with five different mesh sizes for the casing-distributor ensemble: 1.7M (called mesh 1), 4.6M (mesh 2), 8.5M (mesh 3), 11.7M (mesh 4) and 19.5M nodes (mesh 5). Typical computation time for the first four mesh sizes is respectively about 15 min, 60 min, 376 min, and 18 hours using 12 processors, and 16 hours for the largest mesh size, using 24 processors. Figure 4 shows a comparison of the calculated guide vane torques obtained for the five mesh sizes versus the experimental data. The calculated torque is shown for all guide vanes while the experimental torque was measured only for vanes 1, 2, 6, 11, 16, and 20 as shown in Fig. 3.

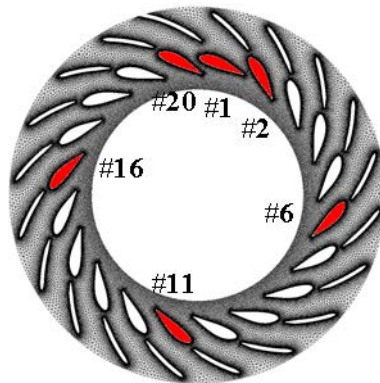


Fig. 3 Guide vane for the experimental torque measurement (in red and numbering 1,2,6,11,16 and 20) for case #1. The distributor is in the same position than in Fig 2 (left).

We find that the numerical results obtained from the five mesh sizes are practically identical and they follow the trend of the experimental data quite well. Similar observations, made for the comparison of the flow angle distribution around the distributor and upstream of the stay vane for five of the mesh sizes, are shown in Fig. 5. Theta is the angle in degrees around the distributor and varies between 0 to 360 degrees. The value $\Theta = 0$ corresponds to the baffle position and increases clockwise. On the other hand, the head losses in the casing and distributor are more sensitive to the mesh refinement. As shown in Table 1 and Fig. 6, the component head losses, expressed as a percentage of total head for a normalized mass flow rate $Q_{11m} = 1 \text{ m}^{0.5} \text{ s}^{-1}$, decrease with larger mesh size. Based on this sensitivity analysis, we have chosen the second smallest mesh size of 4.6M nodes for all flow simulations performed in this paper (mesh 2).

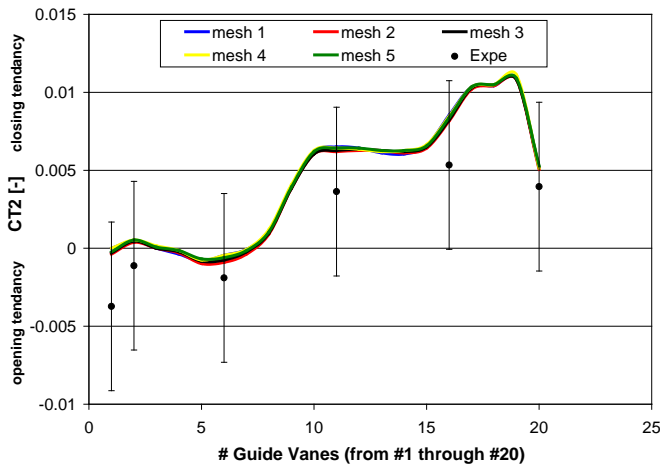


Fig. 4 Torque coefficient CT2 computed with five different mesh sizes

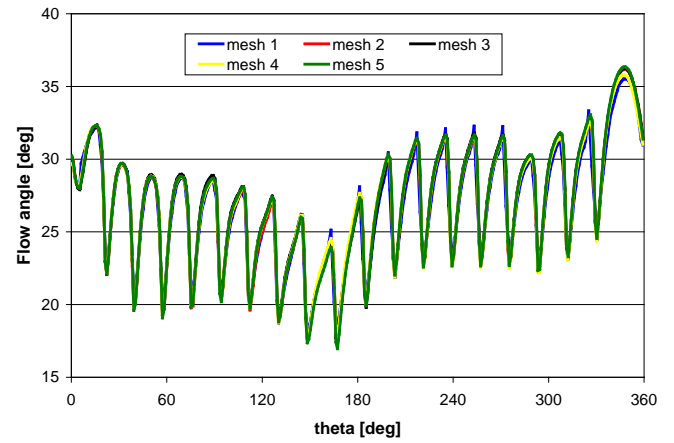


Fig. 5 Flow angle distribution upstream of STV leading edge with five different mesh sizes

Table 1 Comparison of loss for five different mesh sizes

mesh	#1 (1.7M)	#2 (4.6M)	#3 (8.5M)	#4 (11.7M)	#5 (19.5M)
# of nodes Casing	581855	1288260	2811368	3835189	6958654
Casing Loss (% ρgH)	0.8366	0.8084	0.7926	0.7850	0.7824
# of nodes Distributor	1069968	3290658	5639256	7848320	12529766
Distributor Loss (% ρgH)	3.210	2.880	2.837	2.863	2.772

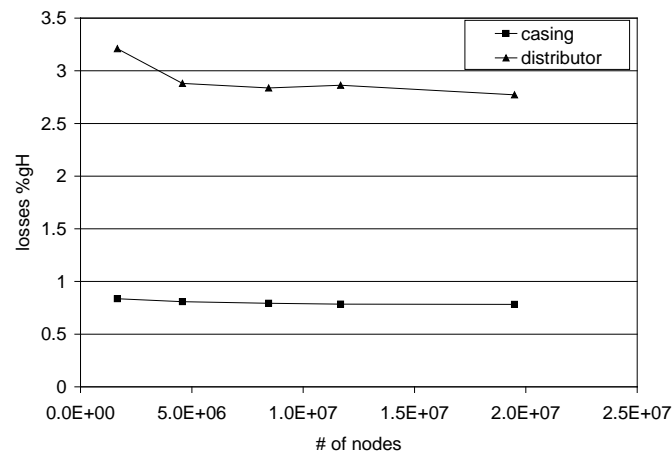


Fig. 6 Losses in % ρgH for casing and distributor in function of number of nodes

5. Torque prediction for synchronized guide vane

5.1 Full 3D distributor case

The computations for synchronized guide vanes are performed for two spiral casings with different distributor height ratios. Spiral casing #1 has 20 guide vanes. In synchronized mode, the guide vane torque is measured for a large range of vane openings: 4°, 8°, 12°, 16°, 20°, 24°, 28°, 32° and 34° for the speed coefficient of $n_{ED} = 0.2937$. Flow simulations are performed for the same tested guide vane openings and the numerical results are compared to the experimental data as shown in Fig. 7. The torque prediction matches the measurements well and it follows the guide vane closing and opening tendencies.

Spiral casing #2 has 24 guide vanes. The flow simulations are performed for guide vane openings of 8°, 12°, 14°, 20°, 25°, 30°, 41°, 42° and 45° for a speed coefficient of $n_{ED} = 0.47$. As shown in Fig. 8, the numerical results agree well with the experimental data. The torque prediction for test case #1 over predicts slightly compared to the measurement at maximum torque and it underestimates for test case #2, but overall simulations for both geometries fall within measurement uncertainty margins.

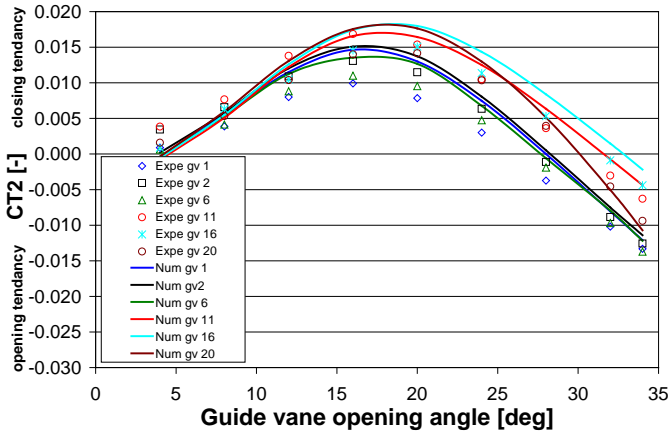


Fig. 7 Torque prediction for individual GV's - Test case #1.

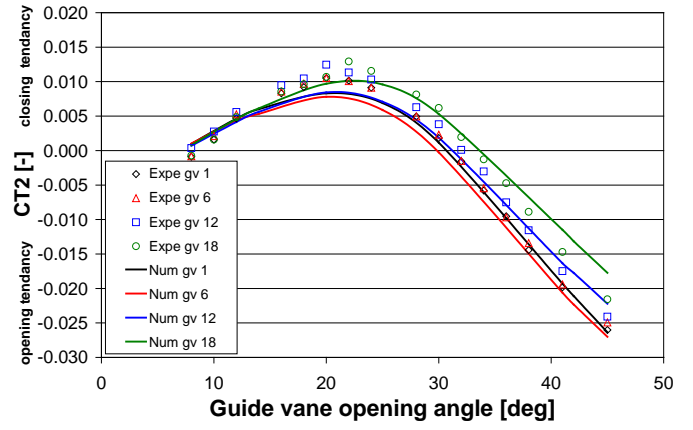


Fig. 8 Torque prediction for individual GV's - Test case #2.

The experimental weighted average guide vane torque coefficient is also compared to the numerical one in Figs. 9 and 10, as Andritz Hydro designers in Pointe-Claire (Canada) typically use these results to evaluate mechanical constraints. The weighted average guide vane torque coefficient is a blend of all CT2 coefficients and is expressed as follows:

$$\langle CT2 \rangle = \frac{(CT2_1 + a_2 CT2_2 + a_3 CT2_3 + a_3 CT2_4 + a_3 CT2_5 + 2CT2_6)}{N_{gv}}, \quad (2)$$

where the coefficient $a_2 = 2$ and $a_3 = 5$ for $N_{gv} = 20$ and $a_2 = 3$ and $a_3 = 6$ for $N_{gv} = 24$, N_{gv} is the total number of guide vanes. A good overall prediction is found and the tendency found in Figs. 7 and 8 are respected.

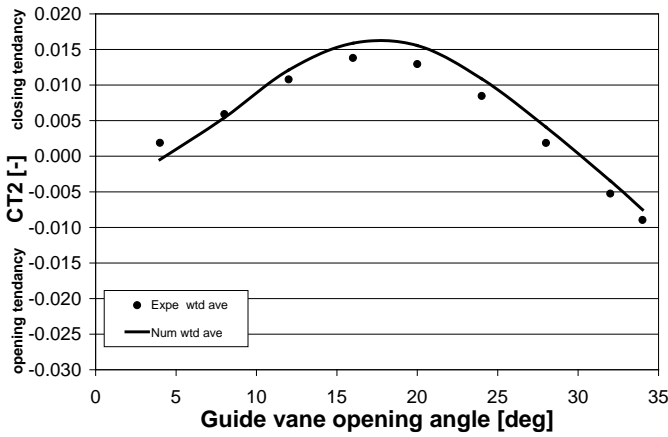


Fig. 9 Average torque prediction - Test case #1.

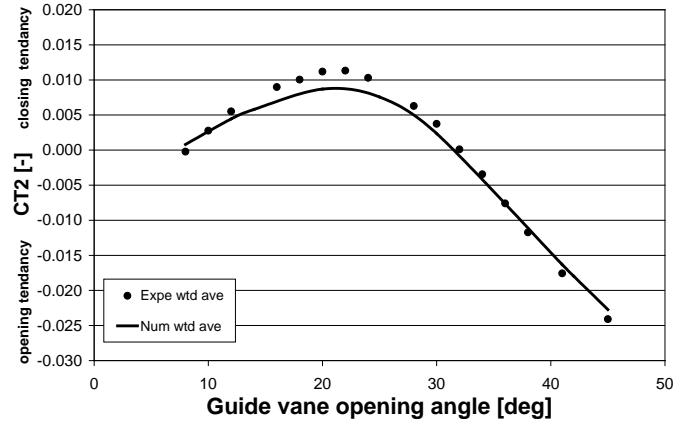


Fig. 10 Average torque prediction - Test case #2.

5.2 Single 2D flow passage distributor case

2D calculations based on the methodology of [11] have been also performed. The 2D mesh and the boundary conditions are shown in Fig. 11. Mass flow rate is imposed at the inlet with a flow angle of 33° . Average static pressure is set at the outlet. Wall boundary conditions are imposed at stay vane and guide vane, symmetric condition is prescribed at the top and the bottom of the domain. Conservative interface flux is set for the periodic boundary conditions. For steady state computations, the convergence criterion was set to 1×10^{-6} on the RMS residuals for all primitive variables. We have imposed a minimum of 100 iterations and a maximum of 300 iterations for all 2D computations. As already mentioned in section 2, the guide vane torque measurement is not performed for all guide vanes in the turbine distributor, but for only a selected few. Moreover, the shape of stay vanes can be different from one passage to another. Two calculations with different stay vanes have been performed for each case. The torque has been evaluated and a comparison between experimental data and 2D and 3D cases is given in Figs. 12 and 13 for the two different geometries. For the first case (Fig. 12), the 2D and 3D cases are very similar and are close to experimental data. For the second case (Fig. 13), the difference is larger for guide vane #6, but a good overall agreement is obtained. At a first stage of design, a 2D approach gives good results for torque estimation.

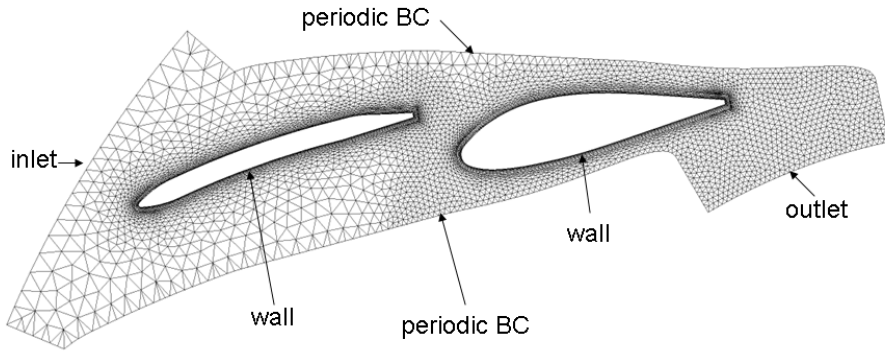


Fig. 11 2D single passage mesh

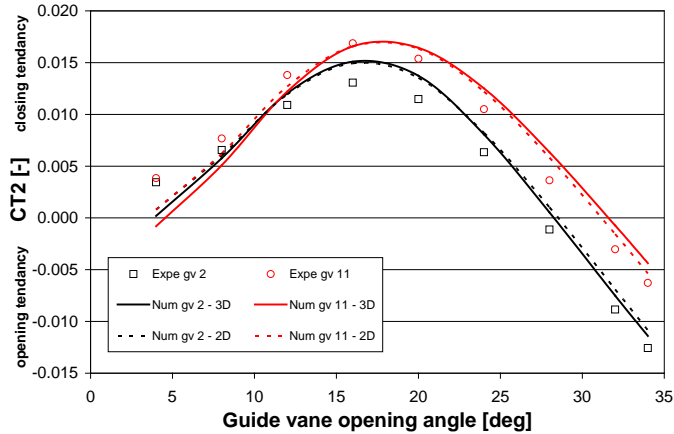


Fig. 12 Torque prediction with 2D and 3D approaches - Test case #1

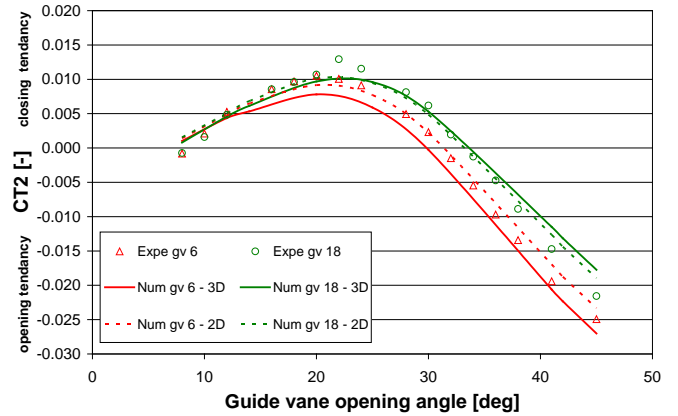


Fig. 13 Torque prediction with 2D and 3D approaches - Test case #2

6. Torque prediction for desynchronized guide vane

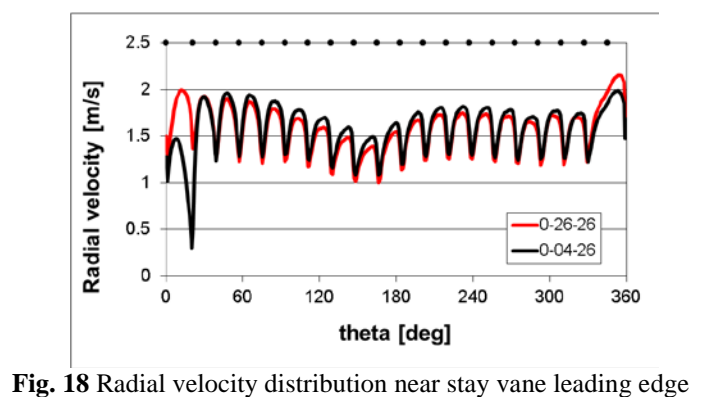
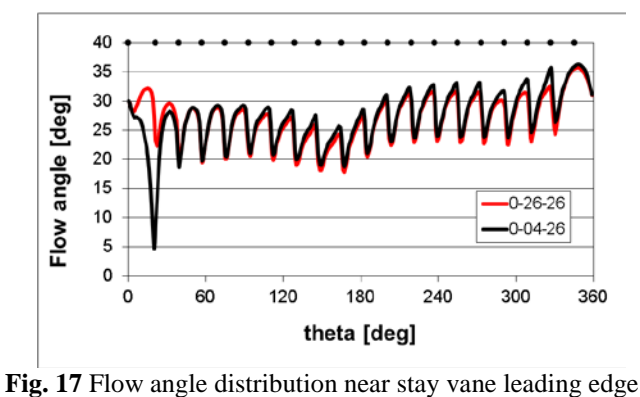
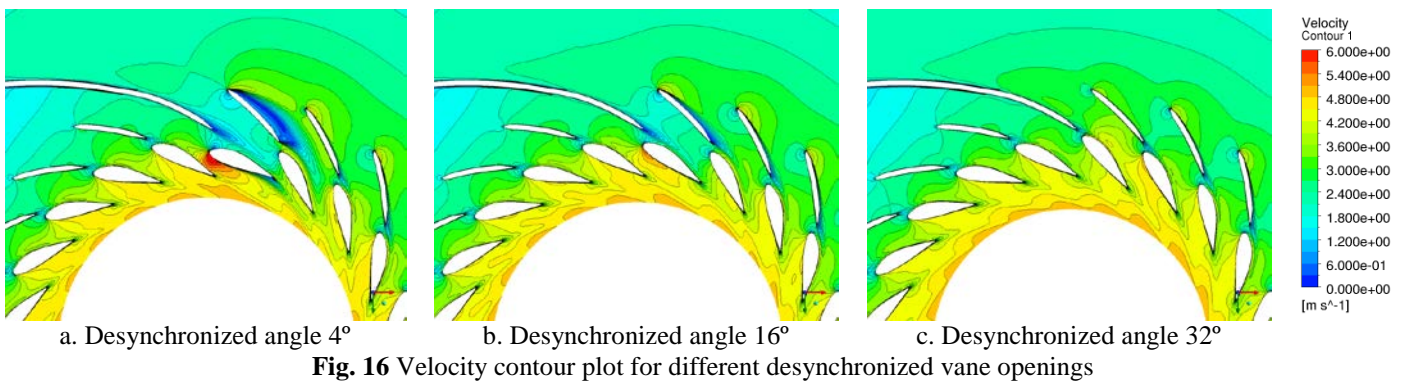
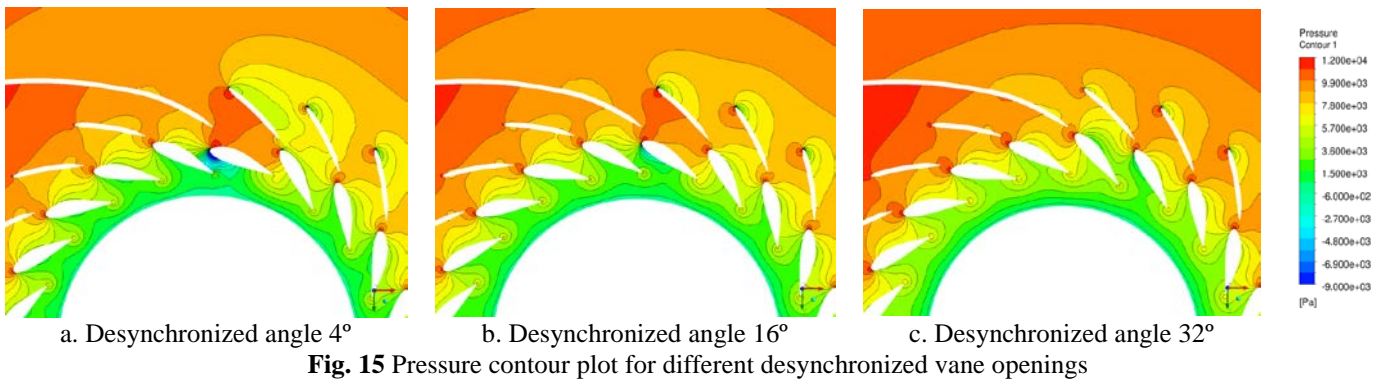
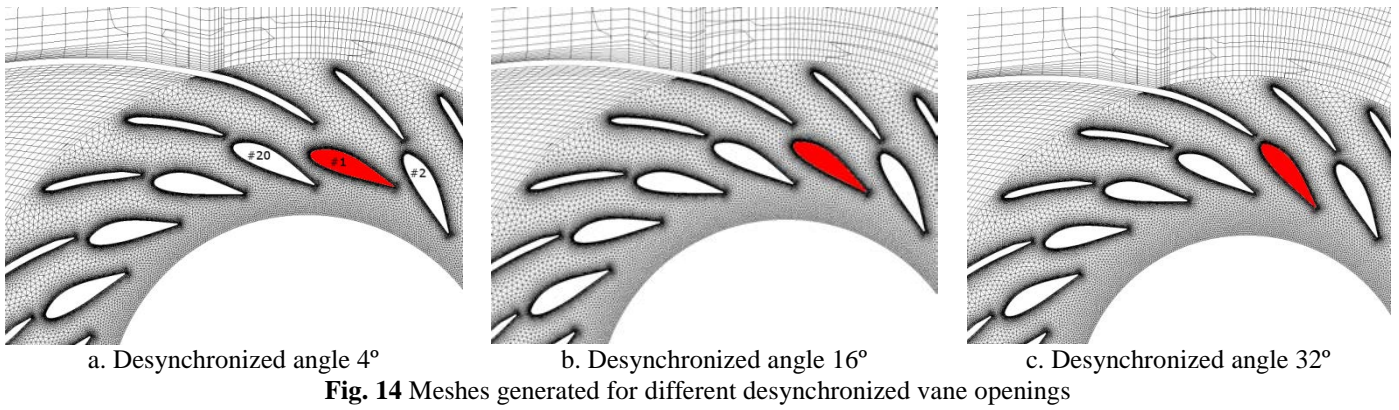
Test case #1 is also used for the desynchronized guide vane torque computation. For experimental investigation of the distributor in desynchronized mode, the guide vane torque measurements are performed for desynchronized guide vane #1, behind the casing baffle, and its two adjacent synchronized guide vanes #20 and #2. The measurement scheme consists of fixing the desynchronized vane in one opening position and varying the other synchronized vanes at different opening positions. For this test case, the desynchronized vane is set for the following 8 fixed positions: 4°, 8°, 12°, 16°, 20°, 24°, 28° and 32° while all other synchronized vane openings vary systematically for 9 vane openings: 4°, 6°, 10°, 14°, 18°, 22°, 26°, 30° and 34°. It takes several days to complete the 72 guide vane torque measurements in the hydraulic laboratory.

The numerical process for computing the guide vane torque of a desynchronized distributor following the same measurement scheme as mentioned above is being captured by a set of scripts. The numerical procedure consists of automatically meshing the casing and distributor, pre-processing, launching the CFD solver and post-processing. The whole process takes less than one hour for a hydraulic engineer to set up the problem and about 20 hours of computation time with mesh #1. For mesh #2, it takes about 72 hours of computation time.

For validation purposes and demonstration of the effect of the desynchronized guide vane on the guide vane torque of the whole distributor, two scenarios of guide vane opening are considered in this study. The first scenario keeps the synchronized guide vanes at a constant opening and varies the desynchronized guide vane opening. The second scenario fixes the desynchronized vane opening and varies the synchronized guide vanes opening. As tested in the laboratory, guide vane #1 behind the baffle is the desynchronized vane in the computations.

6.1 Constant synchronized guide vane opening with different desynchronized openings

In the first scenario, the synchronized guide vanes are kept constant at 26° opening while the desynchronized guide vane is varied by the same opening positions as tested in the lab: 4°, 8°, 12°, 16°, 20°, 24°, 28° and 32°. Figure 14 shows the medium size meshes generated for three desynchronized opening angles of 4°, 16° and 32° with the desynchronized vane in red.



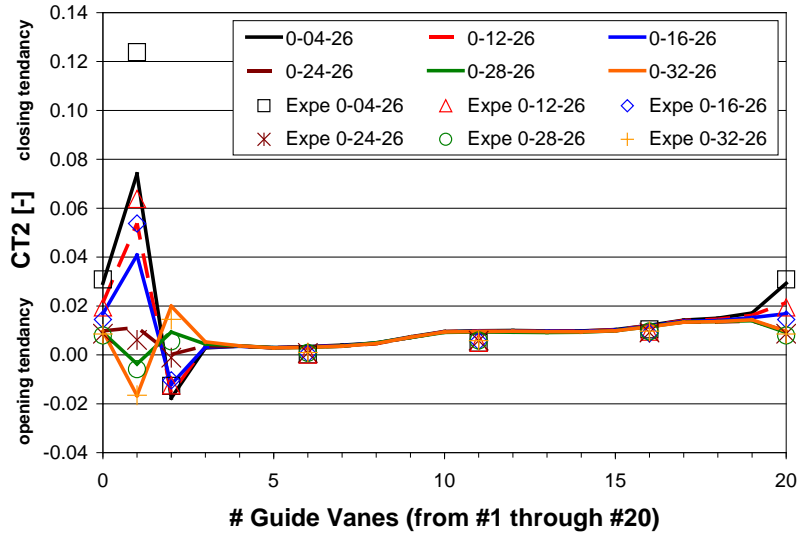


Fig. 19 Torque coefficient CT2 versus guide vane number.
Constant synchronized guide vane opening with different desynchronized openings.

Figure 15 shows the static pressure distribution in the vicinity of the desynchronized guide vane and Fig. 16 the velocity contours. We observe no trace of the GGI interface in the pressure field and the effect of the desynchronized guide vane on the pressure field is very local. In Fig. 16a), a large recirculation zone is observed behind the second stay vane. This recirculation zone vanished as the desynchronized guide vane opening angle increases as shown in Figs 16b) and 16c). Similar observations are made about the flow angle distribution and the radial velocity component distribution upstream of the stay vane leading edge as shown in Figs. 17 and 18. The two figures show a comparison of the flow angle and the radial velocity distribution obtained for a complete 26° synchronized guide vane (symbolised by 0-26-26, in red curve) versus the 26° guide vane opening with a desynchronized vane at 4° (symbolised by 0-04-26, in black curve). For the desynchronized case, there is a sudden drop in the flow angle and the radial velocity vis-à-vis the desynchronized guide vane #1. The points in Figs. 17 and 18 represent the position of the leading edge of each stay vane.

The predicted torque, expressed in CT2, is plotted as a function of the guide vane number for all desynchronized computation cases and is shown in Fig. 19. Since the effect of desynchronized vane #1 is local, only the torques of neighbour guide vanes #2, #3, #19 and #20 vary. Torque values for the synchronized guide vane #20 are repeated in the figure as guide vane #0, to enhance legibility of the figure. The torque on all other guide vanes remains unaffected by the variation of opening of guide vane #1, as they keep the same opening position during all computation cases. The numerical results agree well with the measurement, except for the 4° desynchronized vane opening. For the desynchronized guide vane, downstream of the casing baffle (see Fig. 14a), which receives incoming flow partly from the casing inlet and partly from the casing end, a small numerical error in the flow distribution in the casing itself could cause an imprecision in the desynchronized guide vane torque prediction. In this case, the underestimated torque is caused by an under estimation of the flow rate at the casing end. However, this underestimation is not crucial since the aim of the flow simulation is to predict torque on neighbouring guide vanes of a guide vane blocked by debris, in which case torque on the blocked guide vane is less relevant. As shown in Fig. 19, torque prediction on guide vane #2 and #20 are very well predicted.

6.2 Constant desynchronized opening with different guide vane openings

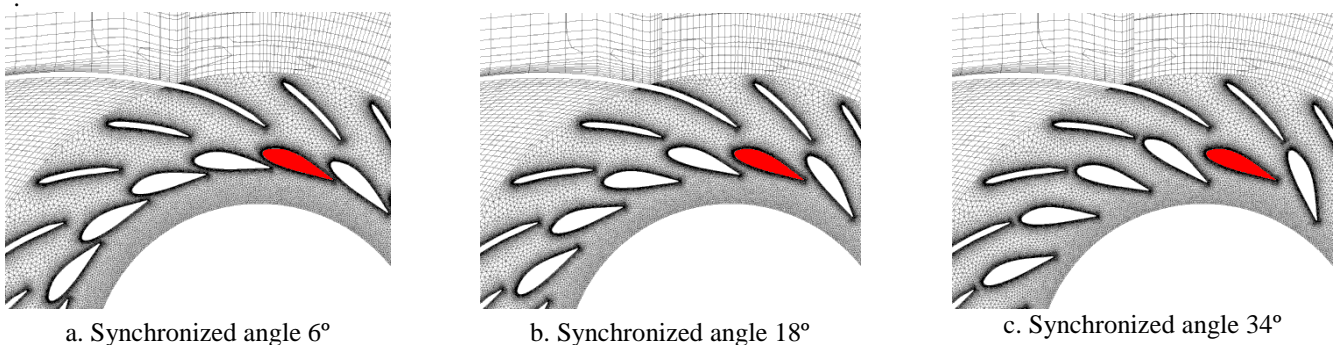


Fig. 20 Meshes for 4° desynchronized guide vane with 3 synchronized guide vane openings.

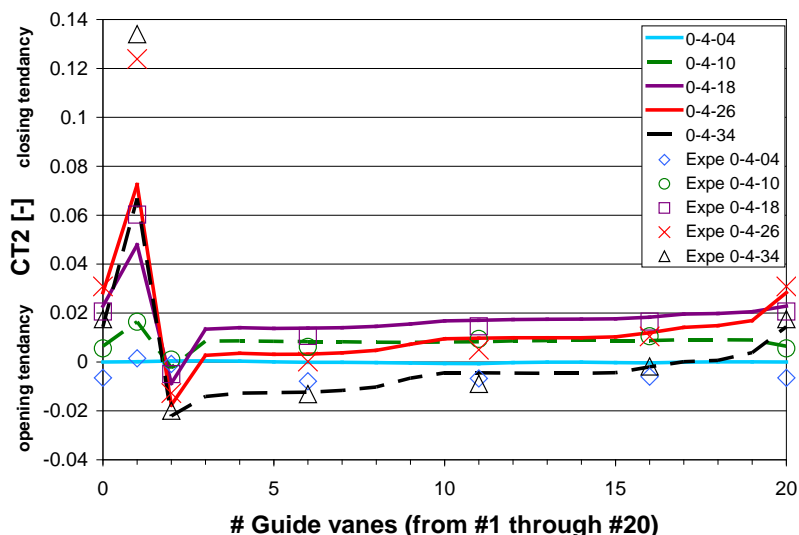


Fig. 21 Torque coefficient CT2 versus guide vane number.
Constant desynchronized opening with different guide vane openings.

In the second scenario, the desynchronized guide vane opening is kept constant at 4° while the synchronized guide vane opening is set respectively to 4° , 10° , 18° , 26° and 34° . As an example, the meshes generated for three synchronized opening angles of 6° , 18° and 34° are shown in Fig. 20. The torque prediction agrees well with the experimental data for all cases as shown in Fig. 21 and it depicts well the sudden change of the guide vane torque in the neighbourhood of the desynchronized vane. As observed in section 6.1, the computed torques of the desynchronized guide vane #1 for case 0-4-26 and case 0-4-34 are underestimated. Comments made in section 6.1 also apply here.

6.3 Attempts to improve results

As shown in Figs. 19 and 21, the torque of the desynchronized guide vane is under-predicted. Additional simulations have been computed in order to better understand that discrepancy. The standard cavitation model of CFX has also been used, but in that case, the predicted torque decreased. Complete steady and unsteady casing, distributor, runner and draft-tube simulations have been computed, but in that case, the torque on the desynchronized guide vane was also decreasing. The $k-\omega$ based Shear Stress Transport (SST) model and the Baseline (BSL) Reynolds Stress model have been used on a fine mesh and results have been improved in the good direction, but not significantly. The under prediction of the desynchronized guide vane torque is still not well understood.

7. Conclusion

In the present paper, a methodology based on CFD to predict guide vane torque in aligned and misaligned configurations has been described. It must be emphasized that the knowledge of a guide vane torque of a distributor in synchronized and desynchronized mode is essential during early stage design.

The laboratory torque measurement procedure has been described and the standard CFD set up has been presented. This numerical procedure, consisting of automatic meshing for the casing and distributor, preprocessing, launching the CFD solver and post-processing, is captured in a set of scripts. It is intended to be used automatically as a design tool. The validation of the guide vane torque prediction for both synchronized and desynchronized modes was carried out with torque measurements obtained from Andritz Hydro's hydraulic laboratory. For synchronized guide vane configuration, 2D and 3D calculations have been performed. It has showed that in general torque predictions agree well with the experimental data. For desynchronized guide vane configuration, similar comments can be made. The flow simulation is able to predict correctly a torque increase on neighbouring guide vanes of a blocked guide vane, except at the desynchronized guide vane itself. This fact was not clearly understood by the authors.

Further validation will be made for semi-spiral casings and also for other operating conditions of the turbine such as runaway condition.

Acknowledgments

The in-house mesh generators used for the study were developed by project Gmath, a joint R&D project between École Polytechnique de Montréal and Andritz Hydro Ltd. The authors would like to acknowledge the National Science and Engineering Council of Canada (NSERC) for its support to the project CRD #386829-09. Thanks are also due to the laboratory team, and in particular to Mr. J. Disciullo, for their contribution with the experimental data base.

Nomenclature

<i>CFD</i>	Computational Fluid Dynamics	HD_{ratio}	Distributor height/throat diameter ratio [-]
<i>CT2</i>	Torque coefficient [-]	H_n	Turbine Head [m]
D_{gv}	Pivot Diameter [m]	N_{gv}	Number of guide vane
G	Gravity [ms^{-2}]	T_{gv}	Torque [Nm]
<i>GGI</i>	General Grid Interface	ρ	Fluid Density [kgm^{-3}]
H_{dist}	Distributor Height [m]		

References

- [1] Mulu Geberkiden, B. and Cervantes, M., 2007, "Effects of Inlet Boundary Conditions on Spiral Casing Simulation," 2nd IAHR International Meeting of the Workgroup on Cavitation and Dynamic Problems in Hydraulic Machinery and Systems, Politehnica University of Timisoara, Timisoara, Romania.
- [2] Oliveira de Souza, L.C.E., Dias de Moura, M., Brasil, A.C.P. Junior and Nilsson, H., 2003, "Assessment of turbulence modelling for CFD simulations into hydro turbines: spiral casings," 17th International Mechanical Engineering Congress, São Paulo, Brazil.
- [3] Maji, P.K. and Biswas, G., 2000, "Analysis of flow in the plate-spiral of a reaction turbine using a streamline upwind Petrov–Galerkin method," International Journal for Numerical Methods in Fluids, Vol 34, No. 2, pp. 113-144.
- [4] Biswas, G., Eswaran, V., Ghai, G., and Gupta, A., 1998, "A numerical study on flow through the spiral casing of a hydraulic turbine," International Journal for Numerical Methods in Fluids, Vol. 28, No. 1, pp. 143-156.
- [5] Xiao, Y.X., Sun, D.G., Wang, Z.W., Zhang, J. and Peng, G.Y., 2012, "Numerical analysis of unsteady flow behaviour and pressure pulsation in pump turbine with misaligned guide vanes," 26th IAHR Symposium on Hydraulic Machinery and Systems, IOP Conf. Series: Earth and Environmental Sciences, Vol 15.
- [6] Liu, J.T., Liu, S.H., Sun, Y.K., Wu, Y.L. and Wang, L.Q., 2012, "Numerical simulation of pressure fluctuation of a pump-turbine with MGv at no-load condition," 26th IAHR Symposium on Hydraulic Machinery and Systems, IOP Conf. Series: Earth and Environmental Sciences, Vol 15.
- [7] Sun H., Xiao, R., Liu, W., and Wang, F., 2013, "Analysis of s characteristics and pressure pulsations in a pump turbine with misaligned guide vanes," ASME Journal of Fluids Engineering, Vol. 135, pp. 1-6.
- [8] Xiao, Y., Wang, Z., Zhang, J., and Luo, Y., 2014, "Numerical predictions of pressure pulses in a francis pump turbine with misaligned guide vanes," journal of Hydrodynamics, Vol. 26, pp. 250-256.
- [9] Roth, S., Hasmatuchi, V., Botero, F., Farhat, M., and Avellan, F., 2010, "Advanced instrumentation for measuring fluid-structure coupling phenomena in the guide vanes cascade of a pump-turbine scale model," Proceedings of the ASME 2010 3rd Joint US-European Fluids Engineering Summer Meeting and 8th International Conference on Nanochannels, Microchannels and Minichannels, FEDSM-ICNMM2010, August 1-5, 2010, Montreal, Canada.
- [10] Grein, H. and Bachmann, P., 1976, "Hydraulic torque on misaligned guide vanes," Water Power and Dam Construction, Vol 28, No. 2, pp.37-40.
- [11] Vu, T.C. and Shyy, W., 1988, "Navier-Stokes Computation of Radial Inflow Turbine Distributor," Journal of Fluids Engineering, Vol 110, pp. 29-32.
- [12] Jost, D. and Velensek, B., 1992, "Numerical prediction of the hydraulic torque on Kaplan turbine guide vanes," American Society of Mechanical Engineers, Fluids Engineering Division, Vol 137, pp. 81-85.
- [13] Vu, T.C., Devals, C., Disciullo, J., Iepan, H., Zhang, Y., and Guibault, F., 2012, "CFD methodology for desynchronized guide vane torque prediction and validation with experimental data," 26th IAHR Symposium on Hydraulic Machinery and Systems, IOP Conf. Series: Earth and Environmental Sciences, Vol 15.
- [14] Dompierre, J., Guibault, F., Dubé, J.-F., Iepan, H. and Vu, T.C., 2007, "Hybrid O-Mesh Generation for Hydraulic Vane Optimization," 10th ISGG Conference on Numerical Grid Generation, Forth, Crete, Greece.
- [15] Guibault, F., Zhang, Y., Dompierre, J., and Vu, T.C., 2006, "Robust and Automatic CAD-based Structured Mesh Generation for Hydraulic Turbine Component Optimization," Proceedings of the 23rd IAHR Symposium, Yokohama, Japan.